Soluble iron nutrients in Saharan dust over the central Amazon rainforest

Joana A. Rizzolo[1], Cybelli G. G. Barbosa[1], Guilherme C. Borillo[1], Ana F. L. Godoi[1], Rodrigo A. F. Souza[2], Rita V. Andreoli[2], Antônio O. Manzi[3], Marta O. Sá[3], Eliane G. Alves[3], Christopher Pöhlker[4], Isabella H. Angelis[4], Florian Ditas[4], Jorge Saturno[4], Daniel Moran-Zuloaga[4], Luciana V. Rizzo[5], Nilton E. Rosário[5], Theotonio Pauliquevis[5], Rosa M. N. Santos[2], Carlos I. Yamamoto[6], Meinrat O. Andreae[4], Paulo Artaxo[7], Philip E. Taylor[8] and Ricardo H. M. Godoi[1]

[1] Environmental Engineering Department, Federal University of Parana, Curitiba, PR, Brazil.
[2] State University of Amazonas - UEA, Meteorology Department, Manaus, AM, Brazil.
[3] Instituto Nacional de Pesquisas da Amazônia, Programa de Grande Escala Biosfera Atmosfera na Amazônia, Manaus, Brasil.
[4] Max Planck Institute for Chemistry, Biogeochemistry Department, Mainz, Germany.
[5] Universidade Federal de São Paulo, Instituto de Ciências Ambientais, Químicas e Farmacêuticas, Diadema, Brasil.
[6] Chemical Engineering Department, Federal University of Parana, Curitiba, PR, Brazil.
[7] Institute of Physics, University of São Paulo, São Paulo 05508-900, Brazil
[8] Deakin University, CCMB and CMMR, School of Life and Environmental Sciences, Geelong, Vic, Australia.

Correspondence to: Philip E. Taylor (philip.taylor@deakin.edu.au) and Ricardo H.M. Godoi (rhmgodoi@ufpr.br).

Abstract. The intercontinental transport of aerosols from the Saharan Desert plays a significant role in nutrient cycles in the Amazon rainforest, since it carries many types of minerals to these otherwise low-fertility lands. Iron is one of the micronutrients essential for plant growth, and its long-range transport might be an important source for the iron-limited Amazon rainforest. This study assesses the bioavailability of iron Fe(II) and Fe(III) in the particulate matter over the Amazon forest, which was transported from the Saharan Desert (for the sake of our discussion, this term also includes the Sahel region). The sampling campaign was carried out above and below the forest canopy at the ATTO site (Amazon Tall Tower Observatory), a near-pristine area in the central Amazon Basin, from March to April 2015. Measurements reached peak concentrations for soluble Fe(III) (48 ng m^{-3}), Fe(II) (16 ng m^{-3}), Na (470 ng m^{-3}), Ca (194 ng m^{-3}), K (65 ng m^{-3}), and Mg (89 ng m^{-3}) during a time period of dust transport from the Sahara, as confirmed by ground-based and satellite remote sensing data and air mass backward trajectories. Dust sampled above the Amazon canopy included primary biological aerosols and other coarse particles up to 12 µm in diameter. Atmospheric transport of weathered Saharan dust, followed by surface deposition, results in substantial iron bioavailability across the rainforest canopy.

The seasonal deposition of dust, rich in soluble iron, and other minerals is likely to assist both bacteria and fungi within the topsoil and on canopy surfaces, and especially benefit highly bioabsorbent species.

35 In this scenario, Saharan dust can provide essential macronutrients and micronutrients to plant roots, and also directly to plant leaves. The influence of this input on the ecology of the forest canopy and topsoil is discussed and we argue that this influence would likely be different from that of nutrients from the weathered Amazon bedrock, which otherwise provides the main source of soluble mineral nutrients.

40 **Key words:** Amazon forest, Amazon Tall Tower Observatory, Saharan dust, mineral nutrients, iron bioavailability, long range transport, primary bioaerosols.

1 Introduction

The Sahara is the largest source of desert dust to the atmosphere (Ginoux et al., 2012). Studies have revealed the extent of the influence of Saharan dust on nutrient dynamics and biogeochemical cycling in

45 both oceanic and terrestrial ecosystems in North Africa and far beyond, due to frequent long-range transport across the Atlantic Ocean, the Mediterranean Sea and the Red Sea, and on to the Americas, Europe and the Middle East (Goudie and Middleton, 2001; Hoornaert et al., 2003, Yu et al., 2015; Longo et al., 2016; Ravelo-Perez et al., 2016; Salvador et al., 2016).

The Amazon Basin, which contains the world's largest rainforest (Garstang et al., 1988; Aragão,

50 2012; Doughty et al., 2015) receives annually about 28 million tons of African dust (Yu et al., 2015), as well as Atlantic sea spray and smoke from African biomass burning (Martin et al., 2010; Baars et al., 2011; Talbot et al., 1990; Andreae et al., 2015). There have been suggestions that Saharan dust transport across the Atlantic may act as a valuable fertilizer of the Amazon rainforest, providing fundamental nutrients to the Amazon forest (Swap et al., 1992; Koren et al., 2006; Ben-Ami et al.,

55 2010; Abouchami et al., 2013). However, little is known about the nutrient amounts reaching the Amazon, their bioavailability, and their potential effect on rainforest ecology. It is, therefore, important to understand the source types, source strengths, and the atmospheric factors that control the solubility of these minerals over the Amazon Basin.

Plants require many nutrients for healthy development (Marschner, 2012). Among several components necessary for plant growth, soluble iron (Fe) is an essential micronutrient (Morrissey and Guerinot, 2009) and it is a key element in several important functions and physiological processes. It participates in chlorophyll functioning and is required for enzymes critical for photosynthesis, such as catalase, peroxidase, nitrogenase, and nitrate reductase (Hochmuth, 2011). Other plant bio-functions, such as respiration and hormonal balance, also require Fe (Pérez-Sanz et al., 1995).

Two distinct pathways have been identified in plant roots for Fe uptake from decomposed litter and weathered bedrock. One, present mainly in dicot plants, reduces Fe(III) to Fe(II) by acidification of the rhizosphere. After this reduction, Fe(II) is transported into cells. In the other pathway, compounds with high affinity for iron are secreted into the rhizosphere, where they react with Fe(III) and form a chelate complex. This complex is moved into cells by specific transporters (Hell and Stephan, 2003; Morrissey and Guerinot, 2009). In the forest, microorganisms such as fungi and bacteria, play a role in nutrient cycling, and often employ multiple distinct iron-uptake systems simultaneously (Philpott, 2006).

Besides iron uptake, other elements are also essential for plants. Magnesium (Mg) and Copper (Cu) are required for photosynthesis and protein synthesis. Calcium (Ca) is essential for cell wall and membrane stabilization, osmoregulation, and as a secondary messenger allowing plants to regulate developmental processes in response to environmental stimuli (Gruzak, 2001). Zinc (Zn) is directly involved in the catalytic function of many enzymes and with regulatory and structural functions (Broadley et al., 2007). Potassium (K) regulates osmotic pressures, stomata movement, cell elongation, cytoplasm pH stabilization, enzymatic activation, protein synthesis, photosynthesis, and transport of sugars in the phloem (Kerbauy, 2012).

Atmospheric mineral dust contributes thousands of tons of minerals to tropical rainforests (Okin et al., 2004; Washington and Todd, 2005; Bristow et al., 2010) and likely contributes to plant nutrition, especially compensating for poor soils with low inherent fertility (Swap et al., 1996). Amazon lowland rainforest soils are shallow and have almost no soluble minerals; added to this, heavy rains readily leach soluble nutrients from the ground, which had been added from litter decomposition and weathered rocks (Koren et al., 2006). There are indications that Saharan desert aerosol can compensate for the poor soils of the Amazon (Gross et al., 2015) with phosphorus (P) contributing as a fertilizer to the forest (Swap et

al., 1992; Okin et al., 2004; Koren, 2006; Bristow et al., 2010; Martin, 2010; Abouchami et. al, 2013; Yu et al., 2015).

Under natural soil conditions, Fe(III) occurs bound to minerals, such as hematite, that are not soluble in water (Isaac, 1997; Zhu, 1997) and Fe dissolution is dependent on the water's ligand capacity as well as on the type and quantity of dust deposited on the surface (Mendez, 2010; Shi et al., 2011). An atmospheric process, particle aging, including photoreduction and proton reactions, controls variations in oxidation state, solubility, and bioavailability of iron oxides in dust and determines the ultimate influence these materials have on environmental and biological processes (Siefert et al., 1994; Reynolds, 2014).

Considering that iron is absorbed by plants as soluble Fe(II) and Fe(III), it is essential to quantify the uptake of this element from long-range transported African dust, and evaluate the potential utilization and effect on the Amazon rainforest as an essential micronutrient. This study aims to assess the bioavailability of Fe(II) and Fe(III) in the particulate matter over the Amazon forest, which was transported from Africa and particularly from the Saharan Desert.

2 Method

2.1 Aerosol sampling

Sampling was performed on a triangular mast (S 2° 08.602', W 59° 0.0033') at the Amazon Tall Tower Observatory (ATTO) site (Andreae et al., 2015), a research area in the central Amazon Basin with minimal influence of anthropogenic emissions, in particular during the wet season when near-pristine atmosphere conditions are prevalent. The sampling period ranged from 19 March to 25 April 2015, which is within the typical season during when dust transport to the Amazon Basin has been reported before (Talbot et al., 1990; Swap et al., 1992; Prospero et al., 2014; Yu et al., 2015). Total particulate matter (TPM) was sampled above the canopy at 60 m height above ground level (AGL) and below the canopy at 5 m height (AGL), and transported in a laminar flow through a 2.5 cm diameter stainless steel tube. The aerosol flow was dried by a diffusion dryer. Atmospheric particles were collected on

polycarbonate filters (47 mm diameter, 0.8 µm pore size, Whatman® Nuclepore) at a flow rate of 10 ± 0.5 L min^{-1}.

Due to different activities at the site, the TPM sampling was performed using the inlet below the canopy (5 m height) for the first 11 days, and the inlet at 60 m height for the other 26 days. Samples were collected over 24 or 48 h periods, in order to accumulate sufficient mass to be quantified by ion chromatography (UV-VIS detection). After sampling, the filters were immediately stored in sterile flasks under refrigeration until laboratory analysis. Each flask contained nitric acid solution (re-filtered HNO$_3$, 99.5%) at pH 2.2 ± 0.3, in order to quench the equilibrium process between the two iron oxidative states, Fe(II) and Fe(III), and to stabilize the iron concentrations (Siefert, 1998, Bruno et al., 2000, Cwiertny et al., 2008, Trapp et al., 2010).

Some additional samples for X-ray Fluorescence (XRF) analysis were collected at the ZF2 site (S 2° 35.984', W 60° 12.617') in the Amazon rainforest, about 140 km SW of ATTO. Aerosol samples were deposited on 47 mm polycarbonate filters using a Norwegian Institute for Air Research stacked-filter unit. The combination of filters with 0.4 and 8 µm pore sizes allowed the separation between the fine (PM2.5) and coarse (PM10) modes with a flow rate of 17 L min^{-1}.

2.2 Ion chromatography analysis

All the analyses were performed on the TPM soluble fraction. Each sampled filter immersed in nitric acid solution was extracted by an ultrasonic bath for 10 mins. The extract of each sample was filtered through a polyvinylidene difluoride (PVDF) sterile membrane, 0.22 µm pore size with a diameter of 25 mm (Millipore, Merck) and analysed by ion chromatography (ICS 5000, Dionex-Thermo Scientific, USA).

For the transition metal quantification and iron speciation, pyridine-2,6-dicarboxylic acid (PDCA) was used as eluent and 4-2-2-pyridyl resorcinol (PAR) was used as a post-column reagent, stabilized by a PC-10 nitrogen pump. The system flow was 0.3 mL min^{-1} through an IonPac CG5A (2 x 50 mm) guard column, CS5A capillary column (2 x 250 mm) and UV-Vis spectrophotometry with detection at 530 nm (Cardellicchio et al., 1997). For soluble Fe(II), Fe(III), Cu, and Zn the detection limits (USEPA,

1997) were 1.7, 0.4, 1.3, and 4.1 µg L^{-1}, respectively and the expanded uncertainties at the 95% level of confidence (BIPM, 2008) were 3, 42, 46, and 56 %, respectively.

140   For the cation analysis, ultrapure water and methanesulfonic acid (MSA) was used as the eluent at a 20 mM constant concentration, with automatic suppression (CSRS suppressor - 2 mm), and with a 0.33 mL min^{-1} system flow through an IonPac CG-12 guard column (2 x 50 mm) and CS-12 (2 x 250 mm) capillary column. This resulted in a 14 min running time for each injection. For soluble Na, NH_4, K, Mg and Ca the detection limits (USEPA, 1997) were 2.0, 1.3, 0.9, 0.7, and 1.8 µg L^{-1}, respectively, and the

145   expanded uncertainties at the 95% level of confidence (BIPM, 2008) were of 9, 7, 21, 11, and 23 %, respectively.

2.3 X-ray fluorescence analysis

Energy dispersive X-ray Fluorescence analysis was applied for the determination of the aerosol elemental composition using an Epsilon 5, PANalytical B.V. instrument. The X-ray tube anode operates

150   with accelerating voltages of 25–100 kV and currents of 0.5–24 mA, at a maximum power of 600 W. The primary target is Sc/W, and 11 secondary targets (Mg, Al, Si, Ti, Fe, Ge, Zr, Mo, Ag, CaF_2, and CeO_2) can be used for measuring different ranges of elements. A special tridimensional polarized-beam geometry reduces the incidence of spurious scattered radiation from the X-ray tube into the detector, thus reducing the background and allowing the measurement of trace elements at very low

155   concentrations (1–30 ng cm^{-2}). Further analytical details of the EDXRF analysis are given by Arana et al. (2014).

2.4 Aerosol physical properties

Aerosol physical properties were determined at ATTO during the entire campaign at 60 m height. Mass concentration and size distribution were measured by an Optical Particle Sizer (OPS, TSI model 3330;

160   size range: 0.3–10 µm) at 5 min resolution (Andreae et al., 2015). Equivalent black carbon concentrations (BC_e) were obtained by a Multi Angle Absorption Photometer (MAAP, Model 5012, Thermo Electron Group, USA; λ = 670 nm), based on light absorption measurements at 637 nm. An absorption cross section value of 6.6 m^2 g was used for the conversion of measured absorption

coefficients into BC_e concentrations (Petzold et al., 2005). Soot, mineral dust, and biogenic particles are light absorbers (Moosmüller et al., 2009; 2011; Guyon et al., 2004; Andreae and Gelencsér 2006) and may contribute to the observed BC_e signal. The relative contributions of particle sources to BC_e can be investigated by considering the absorption spectral variability, by means of the so called Absorption Ångström Exponent (AAE). Soot from fossil fuel combustion typically shows AAE close to 1.0, while particles impacted by dust emissions show AAE greater than 2 (Bergstrom et al., 2007). Studies indicate that samples impacted by biomass burning aerosols show AAE in the range of 1.5-2.0 (Bergstrom et al., 2007; Rizzo et al., 2011). The spectral dependency of particle absorption coefficients was monitored using a 7-wavelength Aethalometer (Model AE33, Magee Scientific Company, USA, $\lambda = 370, 470, 520, 590, 660, 880$, and 950 nm), compensated for filter loading and multiple scattering effects (Rizzo et al., 2011). Particle scattering coefficients were obtained at three wavelengths using an Integrating Nephelometer (Ecotech, model Aurora 3000), compensated for truncation errors (Müller et al., 2011). All measurements were taken under dry conditions (RH<50%). More details of the instrumentation setup are given by Andreae et al. (2015).

2.5 Characterization of aerosol plume advection

To assess advection of the African aerosol plumes heading towards the Amazon during the sampling period, data from multiple platforms (ground-based and orbital remote sensing and modelling tools) were integrated in a complementary way. Air mass backward trajectories were calculated using the Hybrid Single Particle Lagrangian Integrated Trajectory (HYSPLIT) Model from the NOAA Air Resource Laboratory, USA, (National Oceanic and Atmospheric Administration), indicating the airflow toward the ATTO site (Draxler and Rolph, 2015). Thus, dust source areas were inferred by tracking individual dust plumes back to their place of origin (Schepanski et al., 2012) as well as determining transport paths. Ten-day backward trajectories were calculated at three different heights within the atmospheric boundary layer (50, 500, and 1000 m). Every 24 h from 19 March to 25 April 2015, a trajectory was calculated with a finishing point at the ATTO site (S 2° 08.752', W 59° 00.335'), at 19:00 (UTC) (i.e., 15:00 local time).

To evaluate Saharan dust outbreak events and transport toward ATTO during the campaign, ground-based and satellite remote sensing products and *in situ* measurements of aerosol particle optical properties were integrated with the atmospheric large-scale wind field. The wind field product was taken from the Modern-ERa Retrospective Analysis (MERRA), a reanalysis data based on the Goddard Earth Observing System Data Assimilation System Version 5 (GEOS-5; Rienecker et al., 2011). Ground-based and satellite remote-sensing aerosol optical properties, namely Aerosol Optical Depth (AOD), were obtained, respectively, from aerosol products of the AErosol RObotic NETwork (AERONET, Holben et al., 1998) and of the Moderate-Resolution Imaging Spectroradiometer (MODIS) aboard the Terra satellite (Remer et al., 2005). Given the relevance of biomass burning emissions in both regions, sub-Sahara and Amazonia, fire spots taken from the MODIS Active Fire Product (http://modis-fire.umd.edu/index.php, (Giglio et al., 2006; Roy et al., 2008) were integrated and analysed with the MODIS AOD field to clarify the role of smoke source regions.

Meteorological data were obtained by sensors installed on the 80-m walkup tower at the ATTO site, detailed elsewhere (Andreae et al., 2015). Daily values were calculated for accumulated precipitation and average air temperature.

2.6 Spore samples

A Sporewatch spore sampler (Burkard Scientific Pty Ltd, UK) was operated on the walkup tower at 80 m height for 24 h on 16 separate days between 28 March and 23 April, simultaneously with the TPM sampling. Particles larger than 2 µm diameter were impacted onto an adhesive-coated tape attached to a drum within the sampler. This tape was removed, mounted onto a microscope slide and examined with an Olympus BX60 light microscope with brightfield optics. Line scans were performed to identify fungi, and counts were averaged over 24 h and expressed per cubic meter of sampled air. Images were captured with a Canon D1200 DSLR camera and edited with Image J software (Schneider et al., 2012). Fungal spores, pollen, fern spores, and other coarse bioaerosols were identified morphologically by a certified pollen and spore counter with the US National Allergy Bureau.

3 Results and discussion

3.1 Evidence for the influence of African air mass advection on the Amazonian aerosol properties

The largest deposition of iron occurs downwind of the main deserts of the world - North Africa and the Middle East (Mahowald et al., 2009). Koren et al. (2006) estimated that between November and March, the Bodélé Depression is responsible for most of the dust that is deposited annually in the Amazon.

Backward trajectories (HYSPLIT model) show the arrival of air parcels in Central Amazonia originating from the Sahara and downwind areas of the desert between 3 and 6 April 2015 (Figure 1), when the highest concentrations of soluble Fe(III), Fe(II), Na, Ca, K, and Mg in aerosol samples were recorded at the ATTO site. Moreover, high mass concentrations of coarse mode aerosol were measured during this period (Figure 2).

During the campaign period, three major Saharan dust outbreaks occurred, as identified by the AERONET ground based sunphotometers installed at the West African and sub-Saharan sites of Dakar (14° 23' 38''N, 16° 57' 32''W) and in Ilorin (08° 19' 12''N, 04° 20' 24''E). West Africa is also affected by biomass burning emissions at this time of year (Haywood et al., 2008) and therefore a contribution of biomass burning smoke to the Saharan dust outbreaks is likely. However, the decrease seen in the Angstrom Exponent (AE) as AOD increases at Ilorin (Figure 3) and Dakar (not shown) shows that the air parcels across Saharan and Sub-Saharan West Africa during the three dust outbreaks were dominated by coarse mode particles. It is well established that an increase in AOD associated with a decrease in AE in these regions is highly correlated with the presence of dust plumes, and the opposite, an increase in AE associated with an AOD increase is related to biomass burning plumes (Eck et al.1999; Ogunjobi et al., 2008).

Particulate Fe(III) and Fe(II) concentrations increased between 3 and 9 April, simultaneously with an increase in particle absorption and scattering coefficients (Figure 4.a). A decrease was observed in the intrinsic property, single scattering albedo (SSA, Figure 4.b), suggesting the presence of particles that are efficient light absorbers, such as soot from fossil fuel combustion and biomass burning, mineral dust, and biogenic particles. For comparison, Rizzo et al. (2013) reported that a 7% decrease in SSA at another forest site in the central Amazon during the wet season periods proved to be related to advection of African aerosols. The spectral dependency of absorption, AAE, can be used to distinguish between

the different sources of light absorbing particles. The elevated AAE values observed between 6 and 10 April (Figure 4.b) contradict the influence of soot from fossil fuel combustion. During the clean periods (25 March to 2 April and 16 to 24 April), dominated by biogenic particles, AAE values were around 1.8, so that this source of particles, ever present at Amazonian forest sites, may not have contributed to the AAE increase between 6 and 10 April.

Therefore, two light absorbing particle sources are left to explain the increase in absorption and AAE values: biomass burning and mineral dust particles. Fire activity is typically low in the central Amazon between November and April, with less than 2 fire spots per 1000 km^2 and day on average (Castro-Videla et al., 2013), which is corroborated by the map of fire spots distribution during the campaign period (Figure 5). On the other hand, fires are numerous in sub-Saharan West Africa during the study season, and long-range transport of biomass smoke from this region has been shown to be an important influence on atmospheric composition in central Amazonia during the wet season (e.g., Talbot et al., 1990; Wang et al., 2016). The peak BC_e concentration during this event was 0.3 µg m^{-3}, and assuming that all of the BC_e truly represents black carbon and using a typical mass fraction of 7% BC in savanna fire smoke (Andreae and Merlet, 2001), we can estimate a maximum smoke TPM burden of ca. 4 µg m^{-3} (or about 20% of TPM) during the dust event on 4 April, which compares to a peak mass concentration of 55 µg m^{-3} (details follow in section 3.2).

The dominant role of mineral dust in the aerosol burden during this event can also be corroborated by measurements taken during the same period at another rainforest site (ZF2), ca. 140 km downwind of ATTO. Table 1 shows aerosol element concentrations measured at ZF2 before, during, and after this dust event. The PM10 and BC_e concentrations at ZF2 are in close agreement with those at ATTO, and the soil dust elements Al, Si, and Fe show dramatic increases during the event. A biomass smoke contribution is evident from the increase in fine potassium and BC_e. The rather low fine sulphur concentration is evidence of only a minor influence of fossil fuel derived pollution.

Table 1: Element concentrations in aerosols measured at the ZF2 rainforest site before, during and after the dust event of 3-8 April 2015 (in ng m^{-3}). Potassium and sulphur are in the fine fraction (<2.5 µm), the other concentrations in PM10.

	27 Mar - 02 Apr	03 Apr - 08 Apr	09 Apr -15 Apr
PM10	2900	13700	4800
BC_e	43	271	100
K(fine)	5	97	25
S(fine)	22	164	47
Na(total)	3	125	34
Ca(total)	3	150	28
Al(total)	7	677	115
Si(total)	12	1267	232
Fe(total)	4	402	62
Al/Fe	1.75	1.68	1.85

Biomass burning in Africa could also have contributed some of the observed Fe, but unfortunately, little is known about Fe emissions from savanna fires, and the available data span a wide range. From the work of Gaudichet et al. (1995), one can derive a Fe content of 0.016% in savanna smoke TPM, which, at a peak biomass smoke concentration of 4 μg m^{-3}, would only give 0.6 ng Fe m^{-3}. Using the BC/Fe ratio of ca. 40 from Maenhaut et al. (1996) and the peak BC_e concentration of 0.3 μg m^{-3}, we can estimate ca. 8 ng Fe m^{-3}. Finally, using the Fe emission factor of 0.026 g kg^{-1} d.m. for African savanna fires from Andreae et al. (1998) and the BC emission factor of 0.6 g kg^{-1} from Andreae and Merlet (2001 and updates), we can estimate a peak pyrogenic Fe contribution of 13 ng m^{-3}. This compares to 64 ng m^{-3} of soluble iron (details follow in section 3.3) at the same time, and, given that only a small fraction of the Fe in biomass smoke is likely to be soluble, it is clear that the dominant fraction of soluble Fe comes from the African mineral dust. Insoluble iron is also the main Fe component in the total aerosol, as can be seen by comparing the total Fe concentration of 402 ng m^{-3} during the 3-8 April period with the average soluble Fe concentration of ca. 52 ng m^{-3} measured over the same time.

Our conclusion that African dust dominates the aerosol budget during the dust event is in agreement with Castro Videla et al. (2013), who, based on a five-year study, concluded that peaks in AOD in the central Amazon during the wet season had a significant contribution from coarse mode particles, pointing to a major role of African advection. Besides this, during this second dust outburst event, the wind speed was stronger than during the first event, implying a faster and more efficient particle transport across the Atlantic, counteracting particle deposition and resulting in substantial effects on

particle chemical composition and optical properties at the site. Moreover, at the ATTO site, meteorological scenarios during the days when the increase in Fe(III) and Fe(II) concentrations was observed, between 3 and 9 April, were characterized by warmer conditions and the absence of rainfall (Figure 6), which precludes aerosol wet removal.

3.2 Characterization of particle physical properties

The mass concentration of PM_{10} particles in Amazonia is close to background in most areas throughout the basin during the wet season. Central Amazonia is characterized by a weak influence of anthropogenic emissions and aerosol mass concentrations are low during the wet season - typically 7 µg m^{-3}; even the most impacted areas do not exceed 10 µg m^{-3} due to intensive rain and the corresponding inhibition of biomass burning (Artaxo et al., 2002; Artaxo et al. 2013; Martin et al., 2010). Increased mass concentrations may occur due to African dust events that reach the Amazon forest in this season (Talbot et al., 1990; Martin et al., 2010). The highest hourly PM_{10} concentration recorded during our entire campaign was around 55 µg m^{-3} at the ATTO site (5 April), with a daily average of 23 µg m^{-3} (Figure 2). Previous studies conducted by Worobiec et al. (2007) at a nearby forest site in Balbina, Amazonia, had also detected an abundance of dust particles during the same season (23 to 29 March 1998). Artaxo et al. (2013) observed relatively low concentrations (<0.3 µg m^{-3}) of soil dust elements (Al, Si, Ti, Fe) during the wet season at a forest site in central Amazonia, but acknowledges episodic concentration increases during periods of influence of particle advection from Africa.

For comparison, during Saharan dust events in the Cape Verde archipelago, PM_{10} concentrations often exceed 100 µg m^{-3}. This is a relatively high concentration when compared to the background level of 10-50 µg m^{-3} (Gross et al., 2015). Obviously, a plume has the highest concentrations near the source, so a larger mass of dust is deposited over the Sahara and the adjacent Atlantic than over the Amazon rainforest. Notably, the concentrations at ATTO were still relatively high in view of the large distance from Africa.

The concentrations of equivalent black carbon (BC_e) measured online during this intensive campaign represented on average 1.5% of PM10 mass concentrations, ranging from 0 to 0.3 µg m^{-3}. This range is in agreement with previous reports for BC_e in the wet season at forest sites in the central Amazon

(Andreae et al., 2015; Rizzo et al., 2013; Martin et al., 2010). Episodic increases of BC_e during the wet season have been attributed to advection of biomass smoke from Africa in previous studies (Talbot et al., 1990; Andreae et al., 2015; Rizzo et al., 2013; Wang et al., 2016). Figure 2 and Table 1 show that BC_e concentrations significantly increased regionally during 1-8 April, coinciding with the increase in PM10 and particle soluble fraction concentrations and indicating that some biomass smoke (probably from fires in West Africa) arrived together with the dust as discussed in the previous section.

3.3 Composition of aerosol soluble fraction

During the entire sampling period, soluble Na and NH_4 are the dominant cations, and have the highest variation in concentration. Soluble Zn, Na, and Ca exhibit maximum concentrations of 106, 95, and 93 ng m^{-3}, respectively, at 5 m height. During the sampling period between 3 and 10 April, the soluble elements Na, K, Mg, Ca, Fe(III), and Fe(II) showed peak concentrations of 470, 65, 89, 194, 48 and 16 ng m^{-3}, respectively, at 60 m height. For the rest of the period, the peak values reached 135, 53, 16, 93, and 15 ng m^{-3}, respectively, and no Fe(II) was measureable. Consequently, the first period cited can be indicative of particulate matter contribution from long distances. The soluble fractions for each element above the canopy from 30 March to 25 April are presented in Figure 7.

The peak concentrations are responsible for the high mean values (black square), except for soluble Zn and Fe(II) (Figure 7). The median values (thick line) for soluble Fe(III), Cu, Zn, Fe(II), and Mg are below 10 ng m^{-3}, while for soluble Na, NH_4, K and Ca the median value is between 10 and 50 ng m^{-3}.

At Bermuda, a location that also receives Saharan dust laden air masses on seasonal cycles, soluble iron was, on average, within the same order of magnitude as at the ATTO site, with mean values ranging from 5 to 9 ng m^{-3} (Longo et al., 2016). The iron in African dust has mixed oxidation states at both ATTO and Bermuda, suggesting that the longer the aerosol remains in the atmosphere, the more reduced the iron becomes. The photoreduction of iron during atmospheric transport and variation in the composition of aerosols could explain this trend (Siefert et al., 1994).

During the wet season in the central Amazon Basin, Artaxo et al. (2002), Martin et al. (2010), and Arana and Artaxo (2014) obtained values of total K, Fe, Cu, and Zn in the same range as those found in our investigation. Potassium, Cu, and Zn are considered to be tracer elements of biogenic emissions

from the rainforest. Potassium in submicron aerosols also has a source from vegetation fires and is frequently used as a tracer for biomass burning aerosols (Andreae et al., 1983; Martin et al., 2010, Zhang et al., 2015). Soil dust related elements are typically present at the highest concentrations during the early wet-to-dry season transition (May), as has been shown in previous studies (Pauliquevis et al.,

350 2012; Andreae et al., 2015). This is mainly driven by large-scale atmospheric circulation patterns that favour the transport of dust plumes in a trans-Atlantic airflow from the Sahara and Sahel regions and towards the Amazon Basin (Artaxo et al., 1990; Formenti et al., 2001; Graham et al., 2003; Martin et al., 2010; Baars et al., 2011; Ben-Ami et al., 2012).

    Biogenic aerosols, present above the canopy in the Amazon during the wet season, are overprinted

355 periodically by episodes of intense transatlantic transport, which brings Atlantic marine aerosols in addition to dust and biomass burning emissions (Talbot et al., 1990; Bristow et al., 2010; Andreae et al., 2015). Zhu et al. (1997) studied North African dust entrained in the trade winds over Barbados (Caribbean) in September, and measured Na concentrations of 2.4 to 6.5 µg m^{-3}. Barbados is in a region that receives large amounts of Na-enriched marine aerosols. While these concentrations are higher than

360 those recorded in the present study at ATTO (220 to 470 ng m^{-3}), the co-occurrence of elevated concentrations of Na in the central Amazon with the mineral dust elements, Al, Fe, and Ca, is clear evidence for the marine origin of Na (Talbot et al., 1990). Andreae et al. (1990) and later Pauliquevis et al. (2012) observed a positive correlation between Na and Cl in rainwater in the Manaus region, a strong indication of sea salt reaching Central Amazonia. Pauliquevis et al. (2012) also observed increases in

365 the concentration of total Fe with values reaching 60 ng m^{-3} in the fine mode mostly during February to April in the Amazon Basin, with a seasonal average of 36 ng m^{-3}. They attributed this to episodes of Saharan dust transport.

    The soluble Fe(II) concentrations recorded at ATTO during our sampling campaign (1.6 to 16 ng m^{-3}) were significantly higher than the Fe(II) concentrations of 0.63 to 8.2 ng m^{-3} measured in mineral

370 dust particles collected from the marine atmospheric boundary layer at Barbados (Zhu et al., 1997). In Barbados, only a small fraction of the total iron in aerosol particles was present as Fe(II). For soluble Fe(III), we found concentrations in the range of 1.1 to 48 ng m^{-3}, with the highest concentrations occurring three days in a row (34, 48 and 33 ng m^{-3}). The soluble Fe(III) concentrations were

significantly higher than those reported by Andreae et al. (2015) from earlier measurements at the same site, which had also been made during the wet season and using the same quantification method. Andreae et al. (2015) had measured 1.8 ng m⁻³ of soluble Fe(III) in 120 ng m⁻³ of total Fe at 80 m height.

This soluble Fe(III) is carried in dust particles that can be deposited onto canopy surfaces by dry deposition. The variation of iron oxidation state in Saharan dust during atmospheric transport could be the effect of atmospheric process during the long oceanic transport, as Fe(II) and Fe(III) have variable susceptibilities to photochemical processes (Longo et al. 2016).

Bristow et al. (2010) analysed aerosol samples collected from the Bodélé Depression, Chad, and suggested that the amounts of Fe in some samples likely indicate the presence of ferromagnesian minerals and also reflect the presence of Fe oxides such as goethite and hematite, or Fe sulphate salts that have been detected in Saharan dust. Abouchami et al. (2013), studying the geochemical characteristics of the Bodélé Depression dust source and the relation to transatlantic dust transport to the Amazon Basin, found lower Na, K, Fe, and Ca concentrations in Amazon Basin soil samples than in the Bodélé samples, suggesting that this difference is a reflection of remobilization and loss of these elements by chemical weathering under the hot, wet climate conditions in the Amazon Basin.

3.4 Coarse particles and bioaerosols above the canopy

Sporewatch sample analysis at ATTO showed that coarse particles, pollen, and fungal spores were common at 80 m height during the African dust plume, whereas very few coarse particles (> 2 µm diameter) had occurred in the atmosphere until 2 April. On 3 April at 17:00 (UTC), coarse particles (2 to 10 µm) peaked in number, and were black, hyaline or variously coloured and of irregular shape. The amorphous particles were interspersed with a large diversity of small fungal particles (Figure 8). Fungi that were identified included basidiospores, such as *Ganoderma* and spores from ground-growing coprinoid fungi. Also present were ascospores, asexual conidia, such as *Cladosporium*, and uni- and bi-cellular hyaline conidia. Several small pollen grains from ground-growing herbs of the Apiaceae family were also observed. No moss or fern spores were found. A full quantitative and taxonomic analysis of bioaerosols at select heights above the canopy and throughout the year of 2015 will be reported in a

separate study. All primary biological particles in the sample had a diameter less than 12 µm, similar to adjacent coarse dust particles. At 80 m height, the total fungal count was 1,587 spores per cubic meter of air, averaged over 24 h (2 to 3 April). High concentrations of fungi and other coarse particles persisted in the samples for several days, peaking again at approximately 20:30 (UTC) on 5 April. From the afternoon of 6 April onwards, once again very few particles and only the occasional spore were observed.

A substantial number of coprinoid spores were identified, but only between 2 and 6 April. Coprinoid fungi have not been found in the canopy of rainforests (Mims and Mims, 2004; Prospero et al., 2005; Womack et al., 2015). Instead, they are more common at ground level across arid and temperate zones, consistent with an African source. Otherwise, they might have come from further away in South America, e.g., from clearings in the forest in NE Brazil. Dust from Lake Chad is also rich in bacteria and fungi (Favet et al., 2013). Bacteria are likely to accompany the dust particles, attached to their surface (Yamaguchi et al., 2012; Prospero et al., 2005). We cannot fully compare the bioaerosol to determine an African source because previous studies cultured air samples of viable spores only, and analysed them with high throughput sequencing. Only a few types of fungi were detected at the species level in these studies. It is unknown whether any of the fungi observed in the dust above the Amazon are still viable upon sedimentation onto the forest. Other than during the formation of a Saharan dust plume, smoke plumes are also known to entrain fungi over long distances (Mims and Mims, 2004), so that some of the fungal material could have been introduced by burning in West Africa.

Up to half of all micronutrients in the canopy are stored in epiphytes (Cardelus, 2010). Fungi housed within lichens take advantage of the large surface area provided by their algal co-host, and are one of the most bio-absorbent organisms evolved for uptake of minerals and other nutrients from atmospheric gases and particulates, and from both dry deposition and rainfall. Another type of fungi common within the Amazon canopy are yeasts, such as Saccharomycetes (Elbert et al., 2007; Womack et al., 2015).

During dry weather, as well as during fog and light rain events, dust deposits onto the canopy and impacts directly onto leaves of vascular plants (e.g., trees and vines), as well as epiphytic vascular and non-vascular plants, such as bryophytes (e.g., lichens, mosses and liverworts). Dust also settles onto ferns and fungi within the canopy. Air sampled from 40 m height showed that fungal material was

emitted from the canopy throughout each day and night. The smallest and most metabolically active fungal emissions detected in the canopy included lichens and yeasts (Womack et al., 2015).

Up to 25,000 tons of phosphorus has been calculated as being deposited each year on the Amazon. Meanwhile, a similar amount of phosphorus has been estimated to be leached from rainforest soils (Yu et al., 2015). While much of the emphasis has been on soil chemistry and root absorption, water-soluble minerals, as such as P and K, can also be absorbed by leaves (Hochmuth, 2011). Mineral nutrients, such as Fe, can be absorbed through plant leaves as well (Fernandez and Brown, 2013). Thus, canopy deposition of Saharan dust is likely to provide soluble iron to plants via their leaves, in addition to having an influence on epiphytes and surface microorganisms.

3.5 Iron availability

The soluble iron measured during the sampling period consisted of about 87% Fe(III) and only 13% Fe(II), and the +II oxidation state was only measurable in four samples. As shown above, soluble iron accounts for only about 13% of total iron during the dust event. The aerosol iron solubility is a key factor in the formation of reactive oxygen species in the aqueous phase (Longo et al., 2016). The pH of the environment is important for solubility and therefore the availability of iron to microorganisms, as more iron is available in acid soils (Isaac, 1997). The majority of Amazon Basin soils are acidic (Schmink and Wood, 1978) and, similar to Fe, Zn is also better absorbed in soils with low pH (Broadley et al., 2007). In contrast, the availability of Zn, Fe and Cu is very low in alkaline soils (Marschner, 2012). However, the efficacy of African dust as a fertilizer depends on many factors, such as particulate matter concentration, composition, solubility, and bioavailability of minerals. In addition, fungi, the most common type of microorganism in the forest (Fracetto et al., 2013), can readily absorb iron, in soluble and insoluble chemical forms.

Iron availability in the canopy of forests has commonly been found to be limiting for growth of epiphytes, bacteria, and fungi (Crichton, 2009). The uptake of iron by plants is more effective through the leaves than the soil (Hochmuth, 2011). In comparison to soil deposition, foliar deposition from dust sedimentation and rainfall washout is likely to be a very effective mode of application for the absorption of soluble iron into the rainforest biota. Therefore, the presence of iron-rich aerosols deposited onto the

canopy is likely to at least partially counter the effects of deficiency of this micronutrient. The majority of soluble mineral nutrients in the Amazon basin soil originated from the gradual weathering of bedrock (Abouchami et al., 2013). Thus, the full extent of the influence of Saharan dust is yet to be determined.

4 Conclusion

460 Peaks in soluble Fe(III) in atmospheric samples at the ATTO tower were traced to a major dust transport event from the Sahara Desert in 2015. Variations in the oxidation state of Fe suggested that a reductive process is taking place during atmospheric transport.

Analyses included meteorological (backward trajectories and wind field), remote sensing (aerosol optical depth), and *in situ* data collection. Biomass-burning aerosols and primary biological particles 465 accompanied the plume at its peak. The contribution of marine aerosols from the Atlantic Ocean was identified by a peak in Na. The ongoing deposition of Saharan dust across the Amazon rainforest provides an iron-rich source of essential macronutrients and micronutrients during the wet season.

Author contribution

470 All authors contributed to the work presented in this paper. R.H.M. Godoi, C.G.G. Barbosa, J.A. Rizzolo, A.F.F. Godoi, C. Pöhlker and A.O. Manzi developed the concept, designed the study and the experiments and J. Rizzolo and I.H. Angelis carried them out. C.I. Yamamoto, G. Borillo and A.O. Manzi provided reagents and gave analytical-technical support. P. Artaxo, C. Pöhlker, J. Saturno, D. Moran-Zuloagal and M.O. Sá collected and analysed data. R.H.M. Godoi, C.G.G. Barbosa, J.A. 475 Rizzolo, P.E. Taylor, L.V. Rizzo, N.E. Rosário, L.V. Rizzo, R.A.F. Souza, R.V. Andreoli, R.M.N. Santos, J. Saturno, D. Moran-Zuloaga, P. Artaxo, M.O. Andreae and T. Pauliquevis analysed data. C. Pöhlker, M.O. Andreae, F. Ditas, L.V. Rizzo, E.G. Alves, T. Pauliquevis and P.E. Taylor gave conceptual advice. J.A. Rizzolo prepared the manuscript and, with contributions from C.G.G. Barbosa, A.F.L. Godoi, E.G. Alves, C. Pöhlker, C.I. Yamamoto, J. Saturno, D. Moran-Zuloaga, L.V. Rizzo, N.E. 480 Rosário, T. Pauliquevis, M.O. Andreae, P.E. Taylor and R.H.M. Godoi, discussed the results and implications at all stages.

Acknowledgments

We acknowledge the support of the Fundação de Amparo à Pesquisa do Estado do Amazonas (FAPEAM), Financiadora de Estudos e Projetos (FINEP), Coordenação de Aperfeiçoamento de Pessoal de Nível Superior (CAPES), Conselho Nacional de Desenvolvimento Científico e Tecnológico (CNPq) and the Fundação Araucária de Apoio ao Desenvolvimento Científico e Tecnológico do Paraná (FA). We acknowledge logistical support from the Central Office of the Large Scale Biosphere Atmosphere Experiment in Amazonia (LBA), the Instituto Nacional de Pesquisas da Amazônia (INPA) and the Universidade do Estado do Amazonas (UEA). We also thank the Max Planck Society and INPA for continuous support. We acknowledge the support by the German Federal Ministry of Education and Research (BMBF contract 01LB1001A) and the Brazilian Ministério da Ciência, Tecnologia e Inovação (MCTI/FINEP contract 01.11.01248.00) as well as the UEA, FAPEAM, LBA/ INPA and SDS/CEUC/RDS-Uatumã. We would like to especially thank all the people involved in the logistical support of the ATTO project, in particular Reiner Ditz and Hermes Braga Xavier. We acknowledge the micrometeorological group of the INPA/LBA for their collaboration concerning the meteorological parameters, with special thanks to Marta Sá and Antonio Huxley. The authors would like to thank Dr. Jose Henrique Pereira from Lawrence Berkeley National Laboratory for the enthusiastic and helpful suggestions.

References

Abouchami, W., Näthe, K., Kumar, A., Galer, S. G., Jochum, K. P., Williams, E., Horbe, A. M. C., Rosa, J. W. C., Balsam, W., Adams, D., Mezger, K. and Andreae, M. O.: Geochemical and isotopic characterization of the Bodélé Depression dust source and implications for transatlantic dust transport to the Amazon Basin, Earth and Planet. Sci. Lett., 380, 112-123, doi:10.1016/j.epsl.2013.08.028, 2013.

Andreae, M. O.: Soot carbon and excess fine potassium: Long-range transport of combustion-derived aerosols, Science, 220, 1148-1151, 1983.

Andreae, M. O., Talbot, R. W., Berresheim, H., and Beecher, K. M., Precipitation chemistry in central Amazonia: J. Geophys. Res., 95, 16,987-16,999, 1990.

Andreae, M. O., Andreae, T. W., Annegarn, H., Beer, F., Cachier, H., Elbert, W., Harris, G. W., Maenhaut, W., Salma, I., Swap, R., Wienhold, F. G., and Zenker, T., Airborne studies of aerosol emissions from savanna fires in southern Africa: 2. Aerosol chemical composition: J. Geophys. Res., 103, 32,119-32,128, 1998.

Andreae, M. O., and Merlet, P., Emission of trace gases and aerosols from biomass burning: Global Biogeochemical Cycles, 15, 955-966, 2001.

Andreae, M. O. and Gelencsér, A.: Black carbon or brown carbon? The nature of light-absorbing carbonaceous aerosols, Atmos. Chem. and Phys., 6, 3131–3148, 2006.

Andreae, M. O., Acevedo, O. C., Araújo, A., Artaxo, P., Barbosa, C. G. G., Barbosa, H. M. J., Brito, J., Carbone, S., Chi, X., Cintra, B. B. L., Silva, N. F., Dias, N. L., Dias-Júnior, C. Q., Ditas, F., Ditz, R., Godoi, A. F. L., Godoi, R. H. M., Heimann, M., Hoffmann, T., Kesselmeier, J., Könemann, T., Krüger, M. L., Lavric, J. V., Manzi, A. O., Lopes, A. P., Martins, D. L., Mikhailov, E. F., Moran-Zuloaga, D., Nelson, B. W., Nölscher, A. C., Nogueira, D. S., Piedade, M. T. F., Pöhlker, C., Pöschl, U., Quesada, C. A., Rizzo, L. V., Ro, C.-U. Ruckteschler, N., Sá, L. D. A., Oliveira Sá, M. C. B., Sales, R. M. N., Santos, J., Saturno, J., Schöngart, M., Sörgel, Souza, C. M., Souza, R. A. F., Su, H., Targhetta, N., Tóta, J., Trebs, I., Trumbore, S., Eijck, A van, Walter, D., Wang, Z., Weber, B., Williams, J., Winderlich, J., Wittmann, F., Wolff, S. and Yáñez-Serrano, A. M.: The Amazon Tall Tower Observatory (ATTO): overview of pilot measurements on ecosystem ecology, meteorology, trace gases, and aerosols, Atmos. Chem. Phys., 15, 10723-10776, doi:10.5194/acp-15-10723-2015, 2015.

Aragão, L. E. O. C.: The rainforest's water pump, Nature, 489, 7415, 217-218, doi:10.1038/nature11485, 2012.

Arana, A. and Artaxo, P.: Composição elementar do aerossol atmosférico na região central da Bacia Amazônica, Química Nova, 37, 268-276, 2014.

Arana, A., Loureiro, A. L., Barbosa, H. M. J., Van Grieken, R., and Artaxo, P., Optimized energy dispersive X-ray fluorescence analysis of atmospheric aerosols collected at pristine and perturbed Amazon Basin sites: X-Ray Spectrometry, 43, 228-237, doi:10.1002/xrs.2544, 2014.

Artaxo, P. and Maenhaut, W.: Trace element concentrations and size distributions of biogenic aerosols from the Amazon Basin during the wet season, Nucl. Instrum. Methods Phys. Res., 49, 366-371, doi:10.1016/0168-583X(90)90277-2, 1990.

Artaxo, P., Gerab, F., Yamasoe, M. A. and Martins, J. V.: Fine mode aerosol composition at three long-term atmospheric monitoring sites in the Amazon Basin, J. Geophys. Res., 99, 22,857-22,868, doi:10.1029/94JD01023, 1994.

Artaxo, P., Martins, J. V., Yamasoe, M. A., Procópio, A. S., Pauliquevis, T. M., Andreae, M. O., Guyon, P., Gatti, L. V. and Leal, A. M. C.: Physical and chemical properties of aerosols in the wet and dry seasons in Rondônia, Amazonia, J. Geophys. Res., 107(D20), 8081, doi:10.1029/2001JD000666, 2002.

Artaxo P., Rizzo, L. V., Brito, J. F., Barbosa, H. M. J., Arana A., Sena E. T., Cirino G. G., Bastos W., Martins S. T. and Andreae M. O.: Atmospheric aerosol in Amazonia and land use change: from natural biogenic to biomass burning conditions, Faraday Disc., 165, 203-235, doi:10.1039/C3FD00052D, 2013.

Baars, H., Ansmann, A., Althausen, D., Engelmann, R., Artaxo, P., Pauliquevis T. and Souza R.: Further evidence for significant smoke transport from Africa to Amazonia, Geophys. Res. Lett., 38, 1-6, doi:10.1029/2011GL049200, 2011.

Ben-Ami, Y., Koren I., Rudich Y., Artaxo P., Martin S T., and Andreae M. O.: Transport of North African dust from the Bodélé depression to the Amazon Basin: a case study, Atmos. Chem. Phys., 10, 7533-7544, doi:10.5194/acp-10-7533-2010, 2010.

Bergstrom, R. W., Pilewskie, P., Russell, P. B., Redemann, J., Bond, T. C., Quinn, P. K. and Sierau, B.: Spectral absorption properties of atmospheric aerosols, Atmos. Chem. and Phys. Disc., 7, 10669–10686,
555 doi: 10.5194/acpd-7-10669-2007, 2007.

BIPM.: Evaluation of measurement data – Guide to the expression of uncertainty in measurement JCGM 100:2008 (GUM 1995 with minor corrections), Paris: BIPM Joint Committee for Guides in Metrology, 2008.

Bristow, C. S., Hudson - Edwards, K. A. and Chappell, A.: Fertilizing the Amazon and equatorial
560 Atlantic with West African dust, Geophys. Res. Lett., 37, L14807, doi:10.1029/2010GL043486, 2010.

Broadley, M. R, White, P. J, Hammond, J. P, Zelko, I. and Lux, A.: Zinc in plants. New Phytol., 173, 677-702, doi:10.1111/j.1469-8137.2007.01996.x, 2007.

Bruno, P., Caselli, M., Gennaro, G., Ielpo, P. and Traini, A.: Analysis of heavy metals in atmospheric particulate by ion chromatography, J. Chromatogr A., 888, 145-150, doi:10.1016/S0021-
565 9673(00)00503-3, 2000.

Cardellicchio, N., Ragone, P., Cavalli, S. and Riviello, J.: Use of ion chromatography for the determination of transition metals in the control of sewage-treatment plant and related waters, J. Chromatogr A, 770, 185-192, doi:10.1016/S0021-9673(97)00086-1, 1997.

Cardelus, C. L.: Litter decomposition within the canopy and forest floor of three tree species in a
570 tropical lowland rain forest, Costa Rica, Biotropica, 42, 300-308, doi:10.1111/j.1744-7429.2009.00590.x, 2010.

Castro Videla, F., Barnaba, F., Angelini, F., Cremades, P., & Gobbi, G. P.: The relative role of amazonian and non-amazonian fires in building up the aerosol optical depth in South America: A five year study (2005-2009), Atmos. Res., 122, 298–309, doi: 10.1016/j.atmosres.2012.10.026, 2013.

575   Crichton R.: Inorganic biochemistry of iron metabolism: from molecular mechanisms to clinical consequences, 3rd Ed, Chichester: John Wiley and Sons, pp 461, doi:10.1002/9780470010303, 2009.

Cwiertny, D. M., Baltrusaitis, J., Hunter, G. J., Laskin, A., Scherer, M. M. and Grassian, V. H.: Characterization and acid-mobilization study of iron-containing mineral dust source materials, J. Geophys. Res., 113, D05202, doi:10.1029/2007JD009332, 2008.

580   Doughty, C. E., Metcalfe, D. B., Girardin, C. A. J., Amézquita, F. F., Cabrera, D. G., Huaraca Huasco, W., Silva-Espejo, J. E., Araujo-Murakami, A., Costa, M. C., Rocha, W., Feldpausch, T. R., Mendoza, A. L. M., Costa, A. C. L., Meir, P., Phillips, O. L. and Malhi, Y.: Drought impact on forest carbon dynamics and fluxes in Amazonia, Nature. 519, 78-82, doi:10.1038/nature14213, 2015.

Draxler, R. R. and Rolph, G. D.: HYSPLIT (Hybrid Single-Particle Lagrangian Integrated Trajectory)
585   Model access via NOAA ARLREADY Website, available at: http://www.arl.noaa.gov/ready/hysplit4.html (last access: 15 October 2016), NOAA Air Resources Laboratory, Silver Spring, MD., 2015.

Eck, T. F., Holben, B. N., Reid, J. S., Dubovik, O., Smirnov, A., O'Neill, N. T., Slutsker, I., and Kinne, S.: Wavelength dependence of the optical depth of biomass burning, urban, and desert dust aerosols, J.
590   Geophys. Res., 104, 31333–31349, doi:10.1029/1999jd900923, 1999.Elbert, W., Taylor, P. E., Andreae, M. O. and Pöschl, U.: Contribution of fungi to primary biogenic aerosols in the atmosphere: wet and dry discharged spores, carbohydrates, and inorganic ions, Atmos. Chem. Phys.7, 4569-88, doi:10.5194/acp-7-4569, 2007.

Favet, J., Lapanje, A., Giongo, A., Kennedy, S., Aung, Y., Cattaneo, A., Davis-Richardson, A. G.,
595   Brown, C. T., Kort, R., Brumsack, H., Schnetger, B., Chappell, A., Kroijenga, J., Beck, A., Schwibbert, K., Mohamed, A. H., Kirchner, T., Quadros, P. D., Triplett, E. W., Broughton, W. J. and Gorbushina, A. A.: Microbial hitchhikers on intercontinental dust: catching a lift in Chad, The ISME Journal, 7, 850-867, doi:10.1038/ismej.2012.152, 2013.

Fernandez V. and Brown P.: From plant surface to plant metabolism: the uncertain fate of foliar applied nutrients, Front. Plant Sci., 4, 289, doi:10.3389/fpls.2013.00289, 2013.

Fracetto, G. M., Azevedo, L. C. B., Fracetto, F. J. C., Andreote, F. D., Lambais, M. R. and Pfenning, L. H.: Impact of Amazon land use on the community of soil fungi, Sci. Agric. 70, 2, 59-67, doi:10.1590/S0103-90162013000200001, 2013.

Formenti, P., Andreae, M. O., Lange, L., Roberts, G., Cafmeyer, J., Rajta, I., Maenhaut, W., Holben, B. N., Artaxo, P. and Lelieveld, J..: Saharan dust in Brazil and Suriname during the Large-Scale Biosphere-Atmosphere Experiment in Amazonia (LBA)-Cooperative LBA Regional Experiment (CLAIRE) in March 1998, J. Geophys. Res., 106, 14919-14934, doi:10.1029/2000JD900827, 2001.

Garstang, M., Scala, J., Greco, S., Harris, R., Beck, S., Browell, E. Sacuse, G., Gregory, G., Hill, G., Simpson, J., Tao, W. and Torre, A.: Trace gas exchange and convective transports over the Amazonian rainforest, J. Geophys. Res., 93, 1528-1550, doi:10.1029/JD093iD02p01528, 1988.

Gaudichet, A., Echalar, F., Chatenet, B., Quisefit, J. P., Malingre, G., Cachier, H., Buat-Ménard, P., Artaxo, P., and Maenhaut, W., Trace elements in tropical African savanna biomass burning aerosols: J. Atmos. Chem., 22, 19-39, 1995.

Giglio, L., Csiszar, I., Justice, C.O.: Global distribution and seasonality of active fires as observed with the Terra and Aqua MODIS sensors, J. Geophys. Res. Biogeosciences, 111, G02016, doi:10.1029/2005JG000142, 2006.

Ginoux, P., Prospero, J. M., Gill, T. E., Hsu, N. C. and Zhao, M.: Global-scale attribution of anthropogenic and natural dust sources and their emission rates based on MODIS Deep Blue aerosol products, Rev. Geophys., 50, RG3005, doi:10.1029/2012RG000388, 2012.

Goudie, A.S. and Middleton, N.J.: Saharan dust storms: nature and consequences, Earth-Sci. Rev., 56, 179-204, doi:10.1016/S0012-8252(01)00067-8, 2001.

Graham, B., Guyon, P., Taylor, P. E., Artaxo, P., Maenhaut, W., Glovsky, M. M., Flagan, R. C. and Andreae, M. O.: Organic compounds present in the natural Amazonian aerosol: Characterization by gas chromatography-mass spectrometry, J. Geophys. Res., 108, 4766, doi:10.1029/2003JD003990, 2003.

625 Gross, A., Goren, T., Pio, C., Cardoso, J., Tirosh, O., Todd, M. C., Rosenfeld, D., Weiner, T., Custódio, D., and Angert, A.: Variability in Sources and Concentrations of Saharan Dust Phosphorus over the Atlantic Ocean, Environ. Sci. Technol. Lett., 2 (2), 31-37, doi:10.1021/ez500399z, 2015.

Gruzak, M. A.: Plant Macro- and Micronutrient Minerals Encyclopedia of Life Sciences Nature Publishing Group, doi:10.1038/npg.els.0001306, 2001.

630 Guyon, P., Graham, B., Roberts, G. C., Mayol-Braceroa, O. L., Maenhaut, W., Artaxo, P., and Andreae, M. O.: Sources of optically active aerosol particles over the Amazon forest, Atmos. Environ., 38, 1039-1051, doi:10.1016/j.atmosenv.2003.10.051, 2004.

Haywood, J. M., Pelon, J., Formenti, P., Bharmal, N., Brooks, M., Capes, G., Chazette, P., Chou, C., Christopher, S., Coe, H. and Cuesta, J.: Overview of the dust and biomass-burning experiment and 635 African monsoon multidisciplinary analysis special observing period, J. Geophys. Res.: Atmos., 113(D23), doi:10.1029/2008JD010077, 2008.

Hell, R. and Stephan U. W.: Iron uptake, trafficking and homeostasis in plants, Planta, 216, 541-551, doi:10.1007/s00425-002-0920-4, 2003.

Hochmuth, G.: Iron (Fe) nutrition in Plant U.S. Department of Agriculture, UF/IFAS Extension Service, 640 University of Florida, IFAS Document SL353, 2011.

Holben, B. N., Eck, T. F., Slutsker, I., Tanré, D., Buis, J. P., Setzer, A., Vermote, E., Reagan, J. A., Kaufman, Y. J., Nakajima, F., Lavenu, F., Jankowiak, I. and Smirnov, A.: AERONET - A federated instrument network and data archive for aerosol characterization, Rem. Sens. Environ., 66, 1-16, doi:10.1016/S0034-4257(98)00031-5, 1998.

645 Hoornaert, S., Godoi, R. H. M., and Grieken, R. V.: Single particle characterization of aerosol in the marine boundary layer and free troposphere over Tenerife, NE Atlantic, during ACE-2, J. Atmos. Chem., 46, 271-293, doi:10.1023/A:1026383403878, 2003.

Isaac, S.: Iron is relatively insoluble and often unavailable in the natural environment: How do fungi obtain sufficient supplies?, Mycologist, 11, 41-42, 1997.

650 Kerbauy, G. B.: Fisiologia Vegetal. 2ª ed, Rio de Janeiro: Guanabara Koogan, pp 431, 2012.

Koren, I., Kaufman, Y. J., Washington, R., Todd, M. C., Rudich, Y., Martins, J. V. and Rosen-feld, D.: The Bodélé depression: a single spot in the Sahara that provides most of the mineral dust to the Amazon forest, Environ. Res. Lett., 1, 1-5, doi:10.1088/1748-9326/1/1/014005, 2006.

Longo, A. F., Feng, Y., Lai, B., Landing, W. M., Shelley, R. U., Nenes, A., Mihalopoulos, N., Violaki, 655 K. and Ingall, E. D.: Influence of Atmospheric Processes on the Solubility and Composition of Iron in Saharan Dust, Environ. Sci. Technol., 50 (13), 6912-6920, doi: 10.1021/acs.est.6b02605, 2016.

Maenhaut, W., Salma, I., Cafmeyer, J., Annegarn, H. J., and Andreae, M. O., Regional atmospheric aerosol composition and sources in the Eastern Transvaal, South Africa, and impact of biomass burning: J. Geophys. Res., 101, 23,631-23,650, 1996.

660 Mahowald, N. M., Engelstaedter, S., Luo, C., Sealy, A., Artaxo, P., Benitez-Nelson, C., Bonnet, S., Chen, Y., Chuang, P. Y., Cohen, D. D., Dulac, F., Herut, B., Johansen, A. M., Kubilay, N., Losno, R., Maenhaut, W., Paytan, A., Prospero, J. M., Shank, L. M. and Siefert, R. L.: Atmospheric Iron Deposition: Global Distribution, Variability, and Human Perturbations, Annu. Rev. Mar. Sci., 1, 245-78, doi:10.1146/annurev.marine.010908.163727, 2009.

665 Marschner, H.: Mineral nutrition of higher plants, Academic Press, London, pp 672, 2012.

Martin, S. T., Andreae M. O., Artaxo P., Baumgardner D., Chen Q., Goldstein A. H., Guenther, A., Heald C. L., Mayol-Bracero, O. L., McMurry, P. H., Pauliquevis, T., Poschl, U., Prather, K. A.,

Roberts, G. C., Saleska, S. R., Silva Dias, M. A., Spracklen, D. V., Swietlicki, E. and Trebs I.: Sources and properties of Amazonian aerosol particles, Rev. Geophys., 48, RG2002, doi:10.1029/2008RG000280, 2010.

Mendez, J., Guieu, C. and Adkins, J.: Atmospheric input of manganese and iron to the ocean: Seawater dissolution experiments with Saharan and North American dusts, Mar. Chem., 120, 34-43, doi:10.1016/j.marchem.2008.08.006, 2010.

Mims, S. A. and Mims, F. M.: Fungal spores are transported long distances in smoke from biomass fires, Atmos. Environ., 38, 5, 651-655, doi:10.1016/j.atmosenv.2003.10.043, 2004.

Moosmüller, H., Chakrabarty, R. K. and Arnott, W. P.: Aerosol light absorption and its measurement: A review, J. Quant. Spec. Rad. Trans., 110(11), 844–878, doi: 10.1016/j.jqsrt.2009.02.035, 2009.

Moosmüller, H., Chakrabarty, R. K., Ehlers, K. M. and Arnott, W. P.: Absorption Ångström coefficient, brown carbon, and aerosols: basic concepts, bulk matter, and spherical particles, Atmos. Chem. and Phys., 11, 1217-1225, doi.org/10.5194/acp-11-1217-2011, 2011.

Morrissey, J. and Guerinot, M. L.: Iron uptake and transport in plants: The good, the bad, and the ionome, Chem. Rev., 109, 10, 4553-4567, doi:10.1021/cr900112r, 2009.

Muller, T., Laborde, M., Kassell, G. and Wiedensohler, A.: Design and performance of a three-wavelength LED-based total scatter and backscatter integrating nephelometer, Atmos. Meas. Tech., 4, 1291–1303, doi: 10.5194/amt-4-1291-2011, 2011.

Ogunjobi, K.O., He, Z., Simmer, C.: Spectral aerosol optical properties from AERONET Sunphotometric measurements over West Africa, Atmos. Res., 88, 89-107, 2008.

Okin, G. S., Mahowald, N., Chadwick, O. A., and Artaxo, P., Impact of desert dust on the biogeochemistry of phosphorus in terrestrial ecosystems: Global Biogeochemical Cycles, 18, GB2005, doi:10.1029/2003gb002145, 2004.

Pauliquevis, T., Lara, L. L., Antunes, M. L. and Artaxo, P.: Aerosol and precipitation chemistry measurements in a remote site in Central Amazonia: the role of biogenic contribution, Atmos. Chem. Phys., 12, 4987-5015, doi:10.5194/acp-12-4987, 2012.

695 Pérez-Sanz, A. and Lucena, J. J.: Synthetic iron oxides as sources of Fe in a hydroponic culture of sunflower, In: ABADIA, J. Iron nutrition in soils and plants, Dordrecht: Kluwer Academic, 241-246, doi:10.1007/978-94-011-0503-3_35, 1995.

Petzold, A., Schloesser, H., Sheridan, P., Arnott, W. P., Ogren, J. and Virkkula, A.: Evaluation of Multiangle Absorption Photometry for Measuring Aerosol Light Absorption, Aerosol Sci. and Tech., 39, 40–51, doi: 10.1080/027868290901945, 2005.

700 Philpott, C.: Iron uptake in fungi: A system for every source, BBA-Mol Cell Res., 1763, 7, 636-645, 2006.

Prospero, J. M., Blades, E., Mathison, G. and Naidu, R.: Interhemispheric transport of viable fungi and bacteria from Africa to the Caribbean with soil dust, Aerobiologia, 21, 1-19, doi:10.1007/s10453-004-5872-7, 2005.

705 Prospero, J. M., Collard, F. X., Molinie, J. and Jeannot, A.: Characterizing the annual cycle of African dust transport to the Caribbean Basin and South America and its impact on air quality and the environment, Global Biogeochem. Cycles, 29, 757-773, doi:10.1002/2013GB004802, 2014.

Ravelo-Pérez, L. M., Rodríguez, S., Galindo, L., García, M. I., Alastuey, A. and López-Solano, J.: Soluble iron dust export in the high altitude Saharan Air Layer, Atmos. Env., 133:49-59, 710 doi:10.1016/j.atmosenv.2016.03.030, 2016.

Remer, L. A., Kaufman, Y. J., Tandré, D., Mattoo, S., Chu, D. A., Martins, J. V., Li, R-R., Ichoku, C., Levy, R. C., Kleidman, R. G., Eck, T. F., Vermonte, E. and Holben, B. N.: The MODIS Aerosol Algorithm, Products, and Validation, Journal of the Atmospheric Sciences, Special Section Volume, 62, 947-973, doi:10.1175/JAS3385.1, 2005.

Reynolds, R. L., Cattle, S. R., Moskowitz, B. M., Goldstein, H. L., Yauk, K., Flagg, C. B., Berquó, T. S., Kokaly, R. F., Morman, S. and Breit, G. N.: Iron oxide minerals in dust of the Red Dawn event in eastern Australia, Aeolian Res., 15, 1-13, doi:10.1016/j.aeolia.2014.02.003, 2014.

Rienecker, M. R., Suarez, M. J., Gelaro, R., Todling, R., Bacmeister, J., Liu, E., Bosilovich, M. G., Schubert, S. D., Takacs, L., Kim, G. K., Bloom, S., Chen, J., Collins, D., Conaty, A., Silva, A., Gu, W., Joiner, J., Koster, R. D., Luchesi, R., Molod, A., Owens, T., Pawson, S., Pegion, P., Redder, C. R., Reichle, R., Robertson, F. R., Ruddick, A. G., Sienkiewich, M. and Woollen, J.: MERRA: NASA's Modern-Era Retrospective Analysis for Research and Applications, J. Climate, 24, 3624-3648, doi:10.1175/JCLI-D-11-00015.1, 2011.

Rizzo, L. V., Artaxo, P., Müller, T., Wiedensohler, A., Paixão, M., Cirino, G. G., Arana, A., Swietlicki, E., Roldin, P., Fors, E. O., Wiedemann, K. T., Leal, L. S. M. and Kulmala, M.: Long term measurements of aerosol optical properties at a primary forest site in Amazonia, Atmos. Chem. Phys., 13(17), 2391-2413, doi:10.5194/acp-13-2391, 2013.

Rizzo, L. V., Correia, A. L., Artaxo, P., Procópio, A. S. and Andreae, M. O.: Spectral dependence of aerosol light absorption over the Amazon Basin, Atmos. Chem. and Phys., 11, 8899–8912, doi: 10.5194/acp-11-8899-2011, 2011.

Roy, D. P., Boschetti, L., Justice, C. O. and Ju, J.: The Collection 5 MODIS Burned Area Product - Global Evaluation by Comparison with the MODIS Active Fire Product, Remote Sensing of Environ., 112, 3690-3707, 2008,

Salvador, P., Almeida, S. M., Cardoso, J., Almeida-Silva, M., Nunes, T., Cerqueira, M., Alves, C., Reis, M. A., Chaves, P. C., Artíñano, B. and Pio, C.: Composition and origin of PM10 in Cape Verde: characterization of long-range transport episodes, Atmos. Environ., 127, 326-339, doi:10.1016/j.atmosenv.2015.12.057, 2016.

Schepanski, K., Tegen, I. and Macke, A.: Comparison of satellite based observations of Saharan dust source areas, Remote Sens. Environ., 123, 90-97, doi:10.1016/j.rse.2012.03.019, 2012.

740   Schmink, M. and Wood, C.: Frontier Expansion in Amazonia, University of Florida press, Gainseville, Florida, 1978.

Schneider, C.A., Rasband, W.S. and Eliceiri, K.W.: NIH Image to ImageJ: 25 years of image analysis, Nature Methods, 9, 671-675, 2012.

Shi, Z., Bonneville, S., Krom, M. D., Carslaw, K. S., Jickells, T. D., Baker, A. R. and Benning, L. G.:
745   Iron dissolution kinetics of mineral dust at low pH during simulated atmospheric processing, Atmos. Chem. Phys., 11, 995-1007, doi:10.5194/acp-11-995, 2011.

Siefert, R. L., Johansen A. M. and Hoffmann, M. R.: Measurements of trace metal (Fe, Cu, Mn, Cr) oxidation states in fog and stratus clouds, J. Air & Waste Manage. Assoc., 48, 128-143, doi:10.1080/10473289.1998.10463659, 1998.

750   Siefert, R. L.; Pehkonen, S. O.; Erel, Y. and Hoffmann, M. R.: Iron photochemistry of aqueous suspensions of ambient aerosol with added organic acids, Geochim. Cosmochim. Acta, 58 (15), 3271−3279, 1994.

Swap, R., Garstang, M., Greco, S. Talbot, R. and Kållberg, P.: Saharan dust in the Amazon Basin, Tellus, 44, 133-149, 1992.

755   Swap, R., Garstang, M., Macko, S., Tyson, P., Maenhaut, W., Artaxo, P., Kallberg, P. and Talbot, R.,: The long-range transport of southern African aerosols to the tropical South Atlantic, J. Geophy. Res., 101, 23777–23791, 1996.

Talbot, R. W., Andreae, M. O., Berresheim, H., Artaxo, P., Garstang, M., Harriss, R. C., Beecher, K. M. and Li, S. M.: Aerosol chemistry during the wet season in Central Amazonia: The influence of long-
760   range transport, J. Geophys. Res., 95, 16,955-16,969, 1990.

Trail, F., Xu, H., Loranger. R. and Gadoury, D.: Physiological and environmental aspects of ascospore discharge in *Gibberella zeae* (anamorph *Fusarium graminearum*), Mycologia, 94, 181–189, 2002.

Trapp, J. M., Millero, F. J. and Prospero, J. M.: Trends in the solubility of iron in dust-dominated aerosols in the equatorial Atlantic trade winds: Importance of iron speciation and sources, Geochem. Geophys. Geosyst., 11, Q03014, doi:10.1029/2009GC002651, 2010.

U.S. Environmental Protection Agency. Determination of inorganic anions in drinking water by ion chromatography, Method 300.1. EPA, 1997.

Wang, Q., Saturno, J., Chi, X., Walter, D., Lavric, J. V., Moran-Zuloaga, D., Ditas, F., Pöhlker, C., Brito, J., Carbone, S., Artaxo, P., and Andreae, M. O., Modeling investigation of light-absorbing aerosols in the Amazon Basin during the wet season: Atmos. Chem. Phys., 16, 14,775-14,794, doi:10.5194/acp-16-14775-2016, 2016.

Washington, R. and Todd, M. C.: Atmospheric controls on mineral dust emission from the Bodélé Depression, Chad: The role of the low level jet, Geophys. Res. Lett., 32, L17701, doi:10.1029/2005GL023597, 2005.

Womack, A. M., Artaxo, P. E., Ishida, F. Y., Mueller, R. C., Saleska, S. R., Wiedemann, K. T., Bohannan, B. L. M. and Green, J. L.: Characterization of active and total fungal communities in the atmosphere over the Amazon rainforest, Biogeosciences, 12, 6337-6349, doi:10.5194/bg-12-6337, 2015.

Worobiec, A., Szalóki, I., Osán, J., Maenhaut, W., Stefaniak, E. A. and Grieken, R. V.: Characterization of Amazon Basin aerosols at the individual particle level by X-ray microanalytical techniques, Atmos. Environ., 41, 9217-9230, doi:10.1016/j.atmosenv.2007.07.056 , 2007.

Yamaguchi, N., Ichijo, T., Sakotani, A., Baba, T. and Nasu, M.: Global dispersion of bacterial cells on Asian dust, Sci. Rep., 2, 525, doi:10.1038/srep00525, 2012.

Yu, H., Chin, M., Yuan, T., Bian, H., Remer, L. A., Prospero, J. M., Omar, A., Winker, D., Yang, Y., Zhang, Y., Zhang, Z. and Zhao, C.: The fertilizing role of African dust in the Amazon rainforest: A first

multiyear assessment based on data from Cloud-Aerosol Lidar and Infrared Pathfinder Satellite Observations, Geophys. Res. Lett., 42, 1984-1991, doi:10.1002/2015GL063040, 2015.

Zhang, Z., Engling, G., Zhang, L., Kawamura, K., Yang, Y., Tao, J., Zhang, R., Chan, C. and Li, Y.: Significant influence of fungi on coarse carbonaceous and potassium aerosols in a tropical rainforest, Environ. Res. Lett., 10, 034015, doi:10.1088/1748-9326/10/3/034015, 2015.

Zhu, X. R., Prospero, J. M. and Millero, F. J.: Diel variability of soluble Fe(II) and soluble total Fe in North African dust in the trade winds at Barbados, J. Geophys. Res., 102, 21297-21305, doi:10.1029/97JD01313, 1997.

790
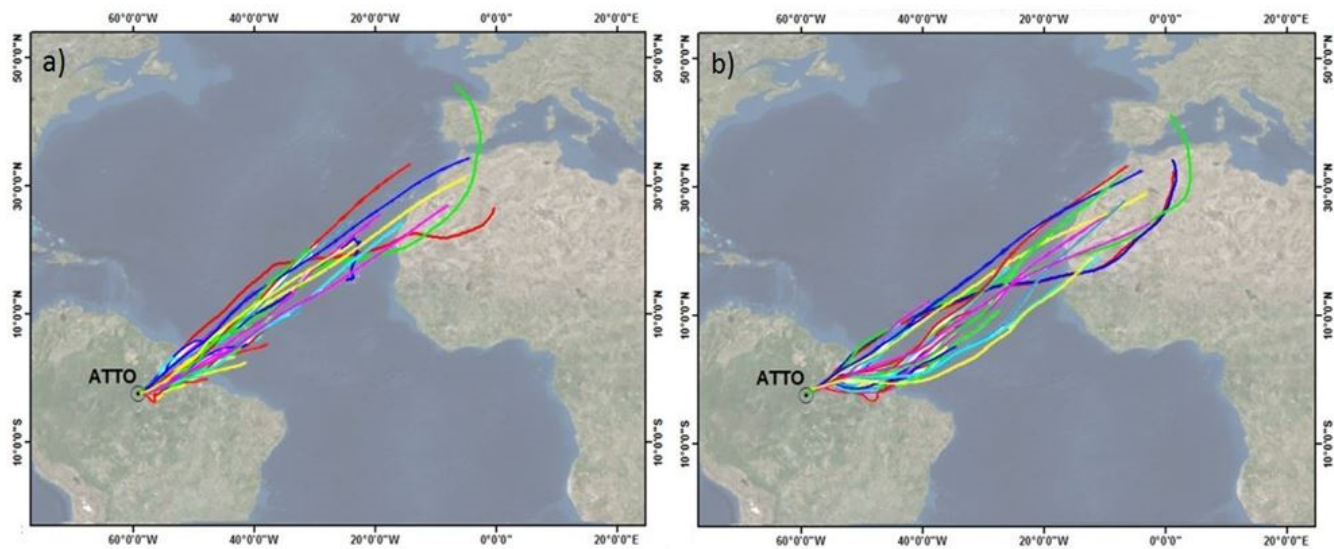
795

Figure 1. Backward trajectories of air parcels above the Amazon for 240 h during the sampling periods for: (a) 5 April 2015 and (b) 6 April 2015, when the greatest concentrations of dust from the Sahara arrived at ATTO.
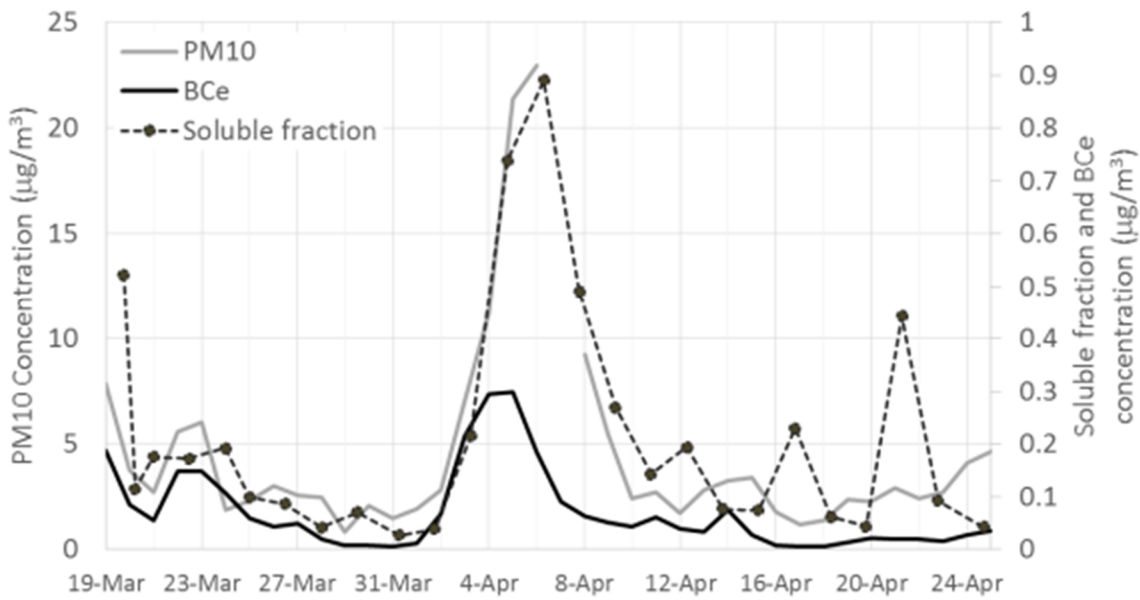
800

Figure 2. Time series of PM$_{10}$ mass concentration, integrated from size distribution measurements (size range: 0.3-10 µm); black carbon equivalent (BCe) concentrations; and total concentration of particle soluble fraction.
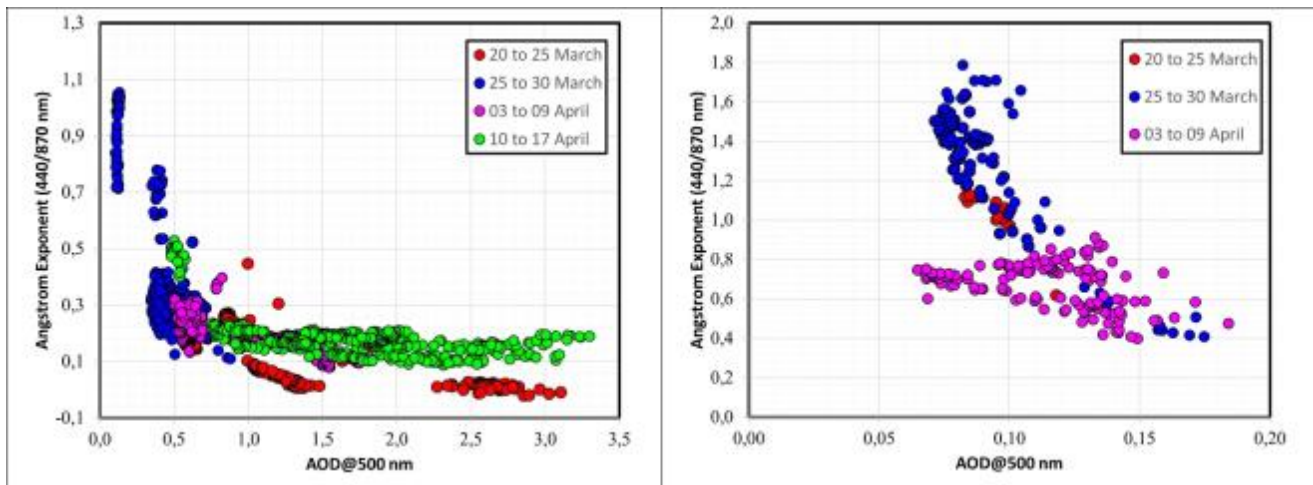
Figure 3. Ångström Exponent (AE) calculated using Aerosol Optical Depth (AOD) from 440 nm and 870 nm as a function of AOD at 500 nm (AOD@500 nm) using data from AERONET sunphotometers installed in Ilorin (08° 19' 12''N, 04° 20' 24''E - left plot) and upwind of Manaus in central Amazonia (02° 53' 12''S, 59° 58' 12''W - right plot) during distinct phases of the sampling period (20 March to 17 April).
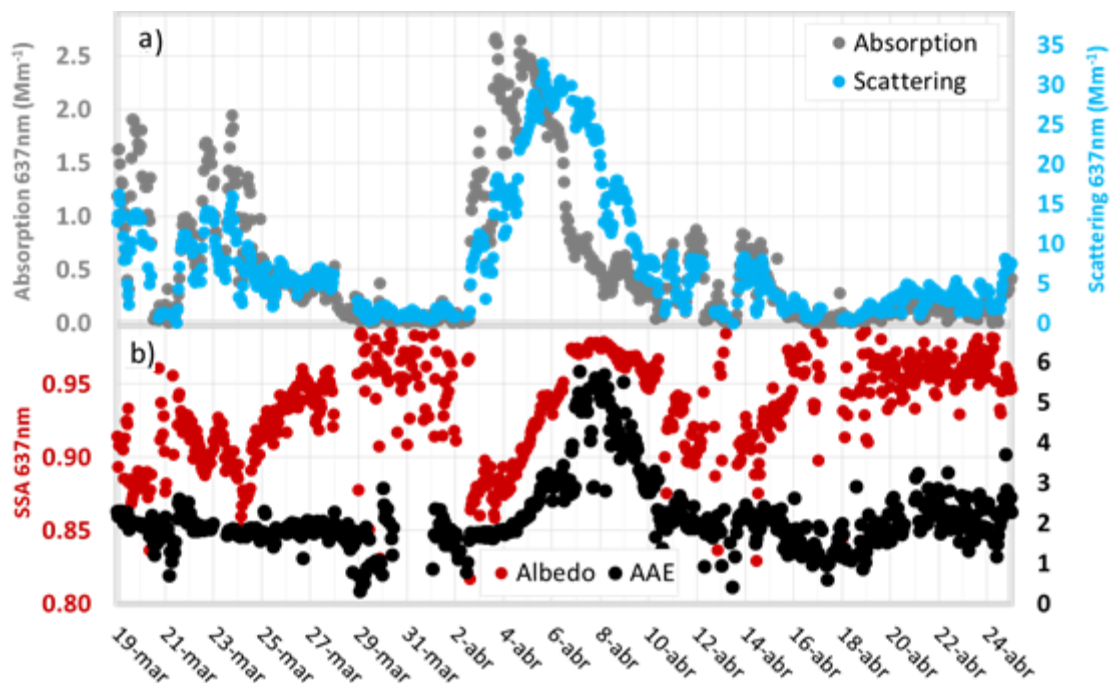
Figure 4. a) Particle absorption and scattering coefficients at 637 nm observed in situ at the ATTO site. b) Particle single scattering albedo (SSA) at 637 nm, and Absorption Ångström Exponent (AAE), retrieved from in situ observations of aerosol optical properties at ATTO.
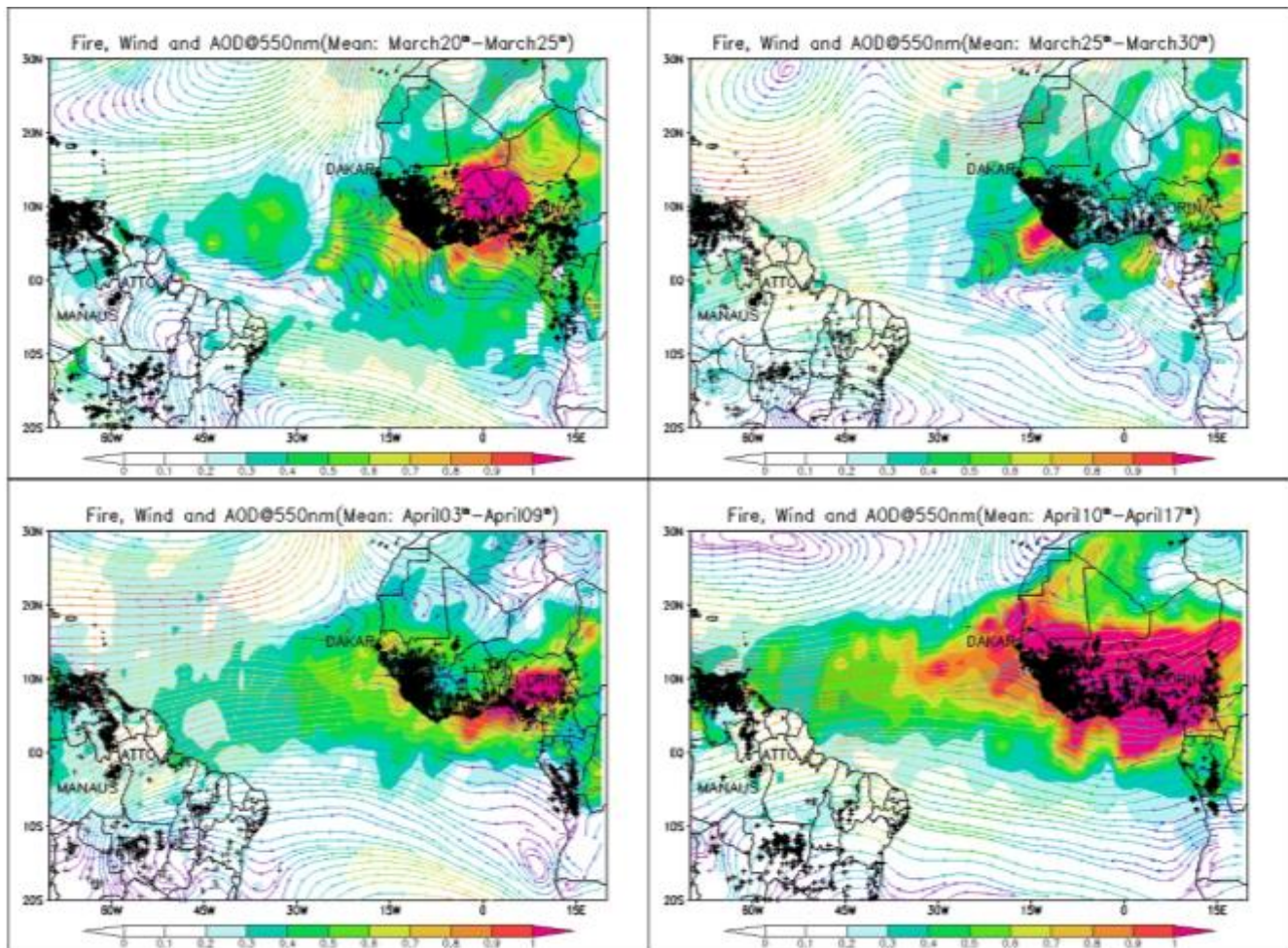
815

Figure 5. Mean aerosol optical depth at 550 nm (AOD, shaded colour) and wind at 850 hPa (stream lines) and total fire spots (black plus symbol) for four distinct periods within the campaign at ATTO site, during the dominance of: a) the first Saharan dust outbreak; b) a less active dust outbreak period; c) the second Saharan dust outbreak; d) the third Saharan dust
820 **outbreak.**
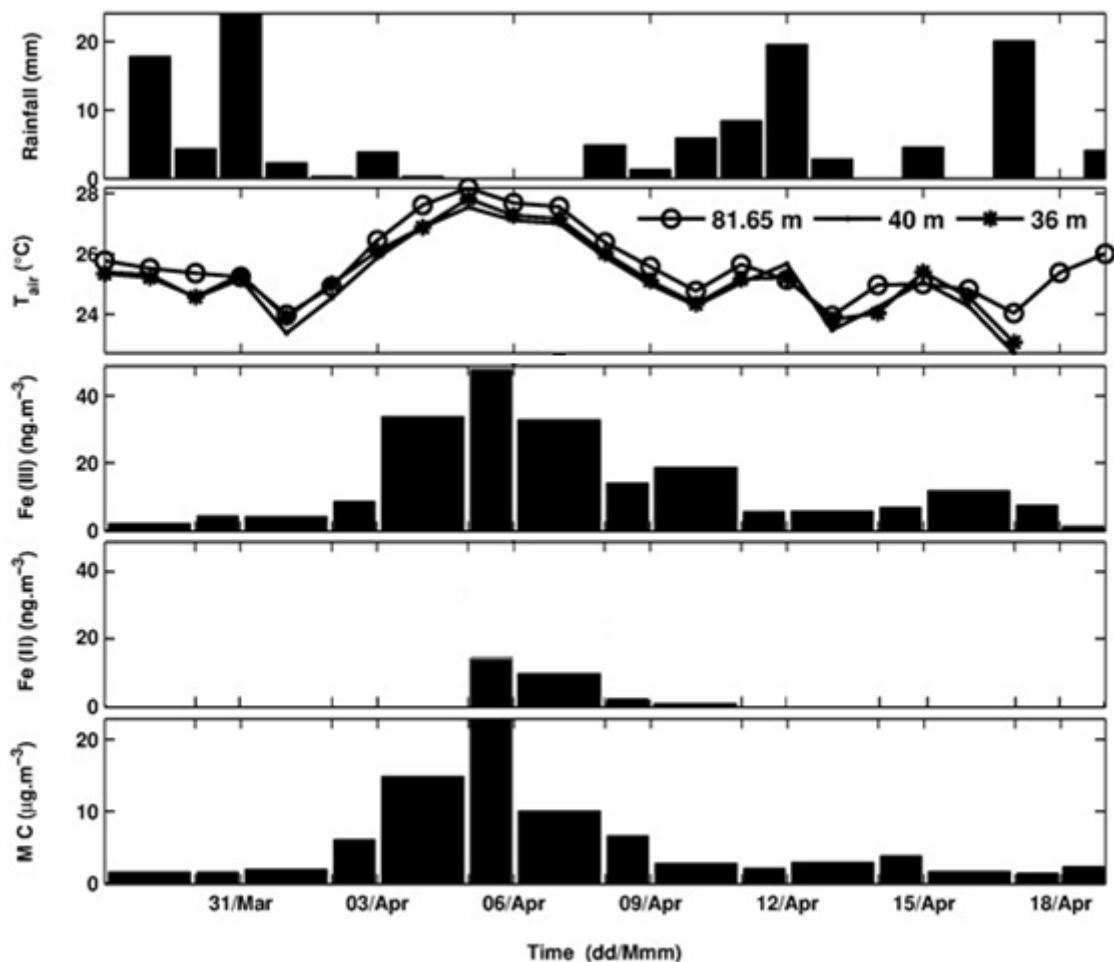
Figure 6. Daily comparison of micrometeorological variables: average air temperature and accumulated precipitation (T$_{air}$, Rainfall) with measurements of soluble Fe(III) and Fe(II) and mass concentration (MC) above the canopy.

825
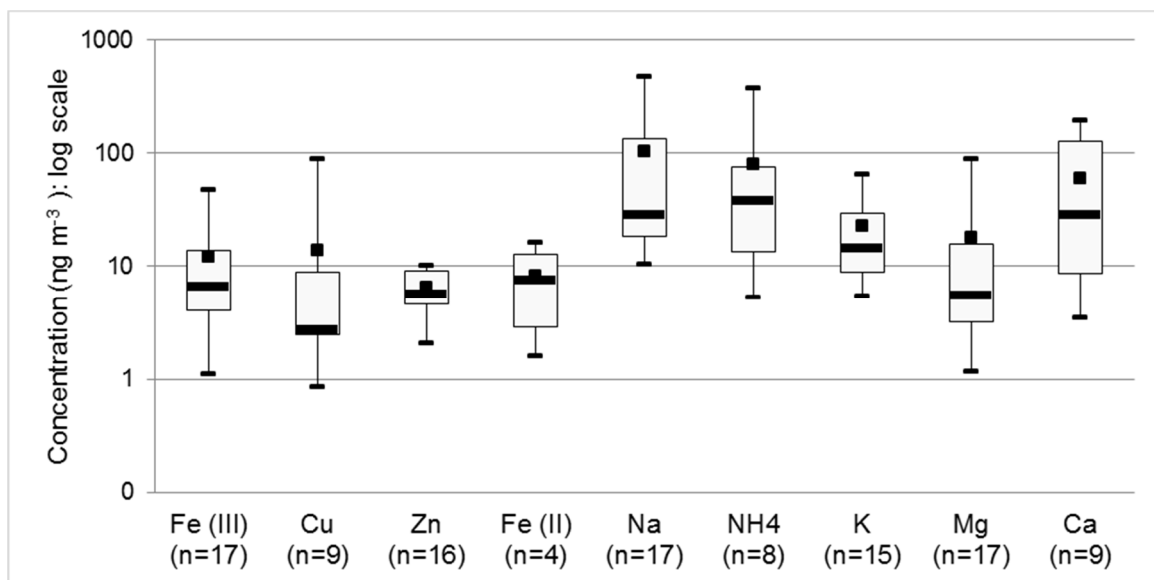
Figure 7. Boxplot for the soluble ion and other species concentrations in the total particulate matter samples at 60 m height from 30 March to 25 April 2015. Upper and lower whiskers represent 1.5 interquartile ranges for the period, upper and lower boundaries are for the third and first quartile. The horizontal bar is the median value and the black square is the average value for each element. In the horizontal axis the number of samples with valid results is shown.

830
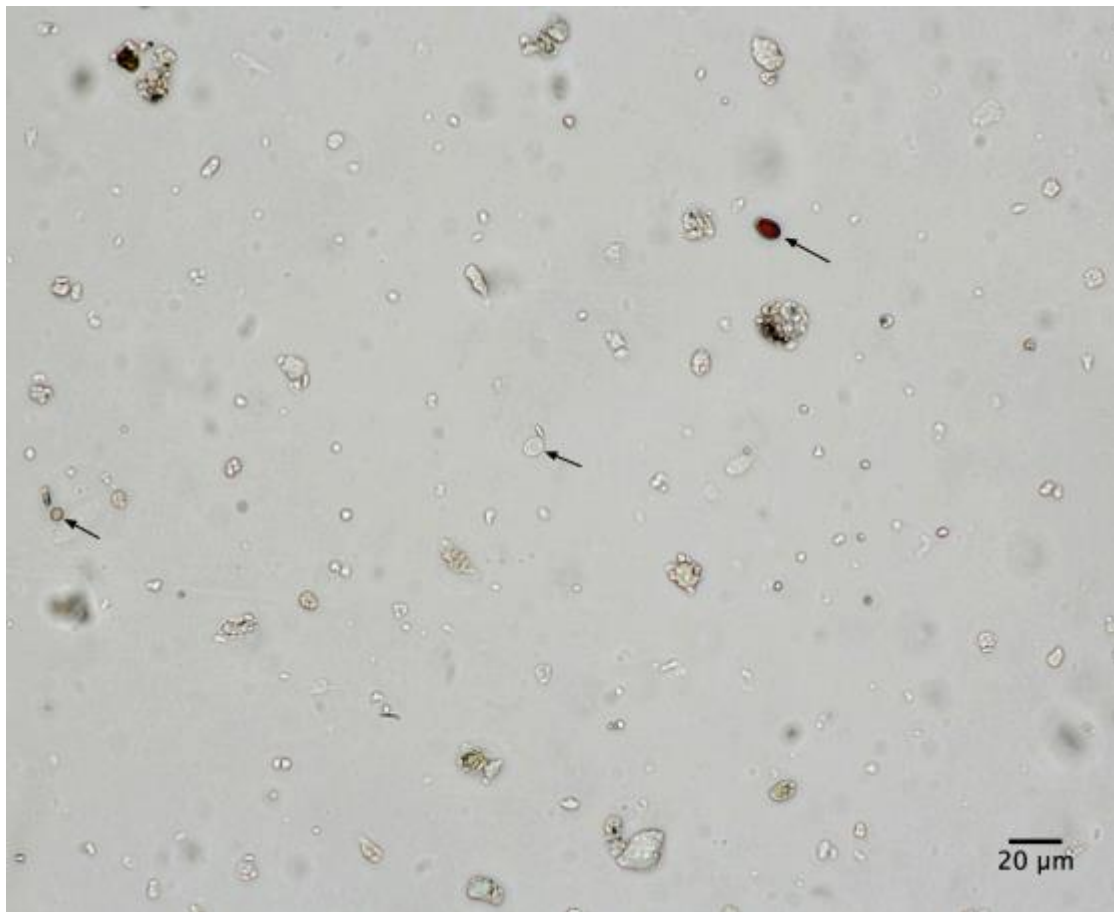
Figure 8. Brightfield microscope image of coarse particles and primary biological particles collected in the air sampler at ATTO at 80 m on 2 April 2015. The arrows point to three fungi: the one on the right is a coprinoid spore, at center is a yeast-like conidia, and at left is a small fungal spore of unknown type.